Acta Cybernetica **26** (2024) 839–854.

Exponential State Enclosure Techniques for the Implementation of Validated Model Predictive Control

Mohamed Fnadi[a] and Andreas Rauh[b]

Abstract

The design task of predictive controllers for uncertain systems is commonly formulated on the basis of their kinematic and/or dynamic models. These models are assumed to be expressed as initial value problems (IVPs) for finite-dimensional sets of nonlinear ordinary differential equations (ODEs). If constraints for the admissible state trajectories are formulated, bounds for these trajectories need to be computed by numerical procedures to obtain guaranteed enclosures of all possible states at each time step that contain the solution of the exact IVP-ODEs. Uncertainties in both the initial states and system parameters are considered in this paper by means of bounded interval variables. For this kind of system representation, we apply an exponential enclosure approach to determine guaranteed enclosures of all reachable states. This approach is embedded in a novel manner into the framework of a guaranteed nonlinear model predictive control (NMPC) to acquire optimal and safe control domains along a receding horizon. The NMPC problem is solved at each time step considering several constraints which are crucial for the system's safety and stability, namely, bounds on the state trajectories and the control signals. The capabilities of the combination of the exponential enclosure technique with the set-based NMPC strategy are illustrated through simulations using a nonlinear inverted pendulum.

Keywords: exponential enclosure, ordinary differential equations, model predictive control, guaranteed numerical integration

1 Introduction

Guaranteed numerical integration is a fundamental tool to solve initial value problems of ordinary differential equations (IVP-ODEs) with uncertain initial conditions

[a]Laboratoire d'Informatique, Signal et Image de la Côte d'Opale – LISIC UR 4491, Université du Littoral Côte d'Opale, F-62228, France. E-mail: mohamed.fnadi@univ-littoral.fr, ORCID: 0000-0001-9593-8859

[b]Carl von Ossietzky Universität Oldenburg, Group: Distributed Control in Interconnected Systems, D-26111 Oldenburg, Germany. E-mail: andreas.rauh@uni-oldenburg.de, ORCID: 0000-0002-1548-6547

DOI: 10.14232/actacyb.302013

and parameters in a reliable and validated way[1]. Providing guaranteed solution enclosures to these IVP-ODEs is essential for designing and verifying linear and nonlinear feedback controllers, mainly for predictive control approaches. In the literature, several validated approaches have been designed for systems with uncertain initial conditions and uncertain parameters to compute state enclosures which are guaranteed to contain all possible IVP-ODEs solutions (under the assumption of correct models and correct bounds of all uncertain parameters involved). For instance, set-valued integration methods exploiting interval Taylor series and Taylor model-based techniques (e.g., the solvers VNODE-LP or COSY VI) were used for the verification of uncertain systems [9, 15]. Moreover, Runge–Kutta schemes (implemented in the DynIbex library) have been used to obtain tight state enclosures [1, 2].

Nevertheless, it has been shown that — due to the computational complexity of Runge–Kutta methods, as used in the previous work of the first author [4] — fast convergence and high accuracy of the computed enclosures are not always guaranteed for finitely long integration time spans, possibly leading to an excessive duration to get the IVP-ODEs' solutions. Similar statements also hold for other state-of-the-art techniques exploiting interval-based methods for solving IVP-ODEs in a guaranteed and validated way (e.g., RealPaver [8], CAPD [10]). This leads to the observation that these solvers may become impractical for the task of control optimization in an NMPC framework due to their high computation time. In other words, fast convergence of this kind of solvers cannot be guaranteed over a finite time and extremely long response times may be exhibited when searching for tight enclosures of the solutions for the problem and hand. To tackle this issue of the computational burden, exponential enclosure techniques for IVP-ODE problems seem to be attractive to remarkably reduce the computing time of validated methods and to approach real-time capability [18, 19]. Compared to Taylor series or Runge–Kutta model-based techniques, the exponential enclosure approach allows contracting the computed state enclosures over time for asymptotically stable dynamics, which prevents growing diameters of the interval enclosures [16]. However, the computed interval bounds may be wider than those determined by alternative, more complex, solution techniques.

The primary goal of an NMPC strategy is to deploy a plant model to predict the system behavior along a receding horizon. At each sampling point, the NMPC technique computes the optimal control input that minimizes a cost function and satisfies all safety constraints (e.g., bounds for the actuator outputs as well as constraints for internal system variables such as position, speed, and acceleration). Among the existing works, real-time, constrained NMPC approaches with safety and stability constraints were proposed in [3, 6], where all constraints are expressed

[1] Due to the fact that these integration routines provide guaranteed state enclosures, they are typically denoted as *verified* in the literature. Throughout this paper, however, we use the term *validated* to point out that the underlying models are approximations to the actual dynamics for which parameters are determined by means of experimental identification. Therefore, a full *verification* of state bounds is not possible but rather only the computation of state enclosures that contain the true reachable sets with a high level of confidence.

in terms of inequalities with respect to the optimization variables. This approach is based on the exact linearization of the nonlinear model so as to formulate the optimization problem completely as a quadratic programming task. Such kind of problem can be handled easily by linear solvers to obtain the optimal control variables. Nevertheless, most of the existing predictive control techniques assume that uncertainties, related to internal parameters of the system model as well as to sensor measurements with bounded accuracy, are neglected. To solve this problem, guaranteed control strategies were developed in recent work to ensure robustness toward all the uncertainties occurring in dynamic parameters. Despite the capability to handle constraints in a reliable manner, they need huge time to compute the state enclosures [4, 14]. The time aspect is especially crucial, because at each sampling instant a validated NMPC needs to compute optimal and guaranteed system inputs along a receding horizon that minimize some interval cost function and ensure compatibility constraints (such as the aforementioned actuator saturations and safety constraints on the state trajectories).

Our motivation is to interface the exponential enclosure techniques published in [18, 19] with the validated NMPC developed in [4], which is based on Runge–Kutta schemes, to remarkably speed up the solution. The NMPC combined with exponential state enclosures will allow to speed up the search for admissible control sequences based on tight enclosures of the dynamic model considering bounded uncertainties on both initial conditions and dynamic parameters. The goal of the proposed controller is twofold: First, a branching procedure enables one to find safe control domains that obey the state constraints and ensure the convergence to reference intervals. Second, the optimization procedure allows the computation of an optimal and point-valued control input that will finally be applied to the system's actuators.

The remainder of this paper is organized as follows. Firstly, an overview of the exponential state enclosure technique is given in Sec. 2. Secondly, Sec. 3 introduces the guaranteed NMPC approach based on interval arithmetic and a validated exponential state enclosure approach. Thirdly, simulation results and discussions are reported in Sec. 4, before Sec. 5 gives conclusions and an outlook on future work.

2 An Exponential Enclosure Technique for Computing Guaranteed Solution Enclosures for IVP-ODEs

Classical numerical integration methods compute approximations of solutions of IVP-ODEs, however, without guarantees on the accuracy of the approximation. Thus, verified approaches have been developed that are supposed to compute guaranteed enclosures of the solution. Firstly, we give an overview of general validated numerical integration methods in Sec. 2.1. Secondly, we present the concept of exponential enclosures in Sec. 2.2. Finally, techniques for stability analysis and an underlying stabilization of open-loop unstable plants are presented in Sec. 2.3 to

achieve a cascaded control architecture that allows for using exponential enclosures efficiently in the frame of NMPC.

2.1 Verified Computation of Enclosures of IVP-ODEs

Consider an uncertain dynamical system defined by the IVP-ODEs

$$\begin{cases} \dot{\mathbf{x}}_t = \mathbf{f}(t, \mathbf{x}_t, \mathbf{u}, \mathbf{p}) \\ \mathbf{x}_0 \in [\mathbf{x}_0] \subseteq \mathbb{IR}^n \\ \mathbf{u} \in [\mathbf{u}] \subseteq \mathbb{IR}^m \\ \mathbf{p} \in [\mathbf{p}] \subseteq \mathbb{IR}^p, \end{cases} \tag{1}$$

where the state vector is denoted by $\mathbf{x}_t$, the vector of dynamic parameters by $\mathbf{p}$, and the control vector by $\mathbf{u}$. The sets $[\mathbf{x}_0] = \left[[x_{10}] \quad \dots \quad [x_{n0}]\right]^T$, $[\mathbf{u}] = \left[[u_1] \quad \dots \quad [u_m]\right]^T$, and $[\mathbf{p}] = \left[[p_1] \quad \dots \quad [p_p]\right]^T$, expressed as interval boxes, are respectively the initial condition of the state vector, the interval-bounded input, and the set of feasible dynamic parameters. This IVP-ODE has a unique solution $\mathbf{x}_t(t, \mathbf{x}_0, \mathbf{u}, \mathbf{p})$ at $t > 0$ since $\mathbf{f} : \mathbb{R} \times \mathbb{R}^n \times \mathbb{R}^m \times \mathbb{R}^p \to \mathbb{R}^n$ is continuous in t and Lipschitz in $\mathbf{x}_t$ (assuming that $\mathbf{u}$ and $\mathbf{p}$ are known and constant). For our purpose, we assume additionally that $\mathbf{f}$ is sufficiently smooth, i.e., of class C^k.

Compared to the classical numerical integration for an IVP-ODE problem, validated approaches consist of solving this problem in a complete and validated way (i.e., each actual solution is rigorously returned and enclosed in a (sufficiently) tight interval). These methods are commonly based on Taylor series [15] or Runge–Kutta methods [2]. Basically, the main principle of validated integration methods is to obtain the tight enclosure of the IVP-ODE problem.

As presented in [1], the purpose of a validated numerical algorithm is to solve Eq. (1) so as to obtain a sequence of boxes $[\mathbf{x}_0], \dots, [\mathbf{x}_K]$ at the time instants $t_0 = 0 < \dots < t_K = T$. At each guaranteed integration step, it is assumed that input and parameter boxes ($[\mathbf{u}_j]$ and $[\mathbf{p}_j]$) are known to compute the state sequences. It is achieved in such a way that the inclusion function, denoted by $[\mathbf{F}]$, satisfies the property

$$[\mathbf{x}_{j+1}] \supseteq [\mathbf{F}]\left(t_j, [\mathbf{x}_j], [\mathbf{u}_j], [\mathbf{p}_j]\right), \ \forall j \in \{0, \dots, K\}. \tag{2}$$

Such approaches work in two stages at each integration step to compute the guaranteed solutions. These steps are:

i) Computation of a *prior* enclosure of the solution $[\tilde{\mathbf{x}}_{j+1}]$, such that for all t in the time interval $t \in [t_j \ ; \ t_{j+1}]$, the inclusion property

$$\mathbf{F}\left(t_j, [\mathbf{x}_j], [\mathbf{u}_j], [\mathbf{p}_j]\right) \in [\tilde{\mathbf{x}}_{j+1}] \tag{3}$$

is satisfied. This stage enables proving the existence and the uniqueness of the solution.

ii) Computation of a *tight* enclosure of the state $[\mathbf{x}_{j+1}]$ at the time instant t_{j+1}, such that $\mathbf{F}\left(t_{j+1}, [\mathbf{x}_j], [\mathbf{u}_j], [\mathbf{p}_j]\right) \in [\mathbf{x}_{j+1}]$. This step makes use of the solution $[\tilde{\mathbf{x}}_{j+1}]$ to bound the *truncation error*, i.e., the distance between the exact solution and the numerical approximation.

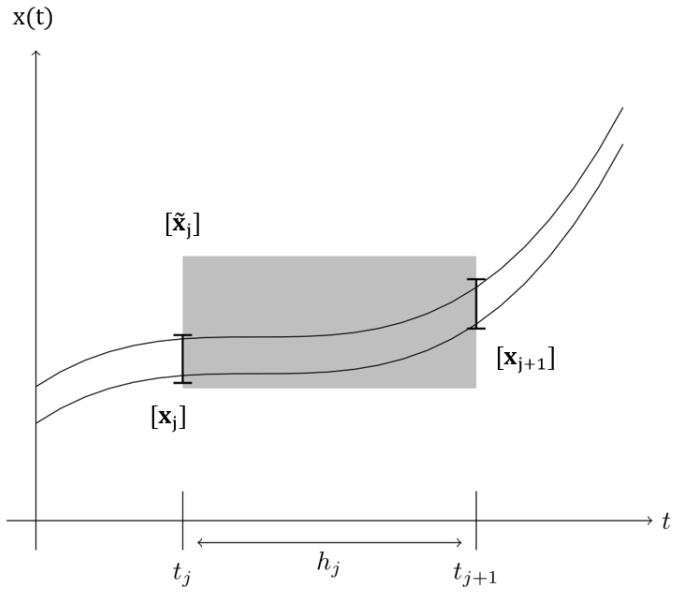

Figure 1: Prior and tight enclosures computed along a single discretization interval using a validated method.

The *tight* and *prior* enclosures calculated along one integration step between t_j and t_{j+1} (step size $h_j = t_{j+1} - t_j > 0$) are visualized exemplarily in Fig. 1.

2.2 Exponential Enclosure Technique

Guaranteed numerical integration methods aim at computing the state enclosure sequence $(t_j, [\mathbf{x}_j])_{j\in\mathbb{N}}$, assuming that the input and parameter boxes $[\mathbf{u}]$ and $[\mathbf{p}]$, respectively, are piecewise constant and known for each run of the validated simulation. To avoid the two-stage evaluation, resulting from a truncated series representation of the solution to the IVP-ODE (1), the exponential enclosure technique [18, 19] is applied to approximate the solutions in a verified manner. It has been shown that this method may improve the accuracy of the computed state enclosures while simultaneously reducing the required computation time for asymptotically stable systems [18, 19].

The dynamic model (1) can be reformulated by considering that the dynamic parameters are represented by constant intervals, and the input variables are assumed to be included in an augmented state vector, i.e., $\left[\mathbf{x}_t^T \quad \mathbf{u}^T(\mathbf{x}_t)\right]^T$, denoted

for brevity again as $\mathbf{x}_t$ with

$$\dot{\mathbf{x}}_t = \mathbf{f}(\mathbf{x}_t). \tag{4}$$

To ensure the (local) asymptotic stability of the system model in the neighborhood of a desired terminal state, we assume — as a prerequisite for the exponential enclosure approach — that a feedback controller $\mathbf{u}_{\mathrm{fb}}(\mathbf{x}_t)$ is included in a cascaded manner in the control law

$$\mathbf{u}(\mathbf{x}_t) = \mathbf{u}_{\mathrm{fb}}(\mathbf{x}_t) + \mathbf{u}_{\mathrm{ff}}(t) \tag{5}$$

so that the NMPC effectively computes a kind of feedforward control sequence $\mathbf{u}_{\mathrm{ff}}(t)$ as shown in Fig. 2.

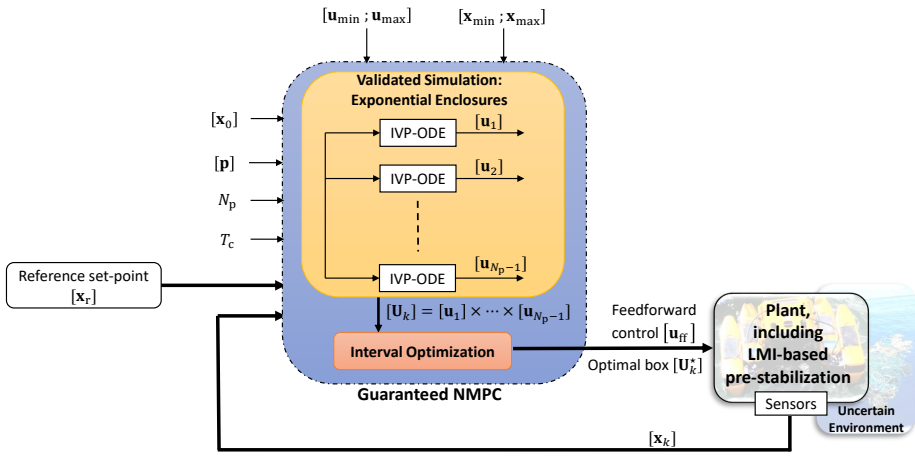

Figure 2: Overall structure of the validated NMPC.

To prevent the growth of the diameters of the intervals $(t_j, [\mathbf{x}_j])_{j\in\mathbb{N}}$ for asymptotically stable systems with a minimum computational effort, the exact solution $\mathbf{x}_t^\star$ can be bracketed by the following exponential state enclosure

$$\mathbf{x}_t^\star \in [\mathbf{x}_e](t) = \exp\Big([\mathbf{\Lambda}]t\Big)[\mathbf{x}_e](0)\ , \quad [\mathbf{x}_e](0) = [\mathbf{x}_0], \tag{6}$$

where $\mathbf{\Lambda}$ represents a yet unknown matrix after a translation of the state space so that the origin $\mathbf{x} = \mathbf{0}$ corresponds of the system's (asymptotically stable) equilibrium. By choosing $[\mathbf{\Lambda}] = \mathrm{diag}\{[\lambda_i]\}$, $i = 1, \ldots, n$, as a diagonal matrix, its elements λ_i need to have negative real parts to describe contracting state enclosures.

Using the exponential state enclosures (6) and a Picard iteration with the iteration index κ, we obtain

$$\begin{aligned}\mathbf{x}_t^\star \in [\mathbf{x}_e]_{(\kappa+1)} &= \exp\Big([\mathbf{\Lambda}]_{(\kappa+1)}\, t\Big)[\mathbf{x}_e](0) \\ &= [\mathbf{x}_e](0) + \int_0^t \mathbf{f}\Big(\exp\Big([\mathbf{\Lambda}]_{(\kappa)}\, s\Big)[\mathbf{x}_e](0)\Big)\,\mathrm{d}s.\end{aligned} \tag{7}$$

The differentiation of (7) with respect to time, belonging to the integration interval $t \in [0\,;\,T]$, leads to

$$\dot{\mathbf{x}}_{[t]}^\star \in [\mathbf{\Lambda}]_{(\kappa+1)} \exp\Big([\mathbf{\Lambda}]_{(\kappa+1)}[t]\Big)[\mathbf{x}_e](0) = \mathbf{f}\Big(\exp\Big([\mathbf{\Lambda}]_{(\kappa)}[t]\Big)[\mathbf{x}_e](0)\Big). \tag{8}$$

Assuming a converging iteration with $[\mathbf{\Lambda}]_{(\kappa+1)} \subseteq [\mathbf{\Lambda}]_{(\kappa)}$ and, thus, $[\lambda_i]_{(\kappa+1)} \subseteq [\lambda_i]_{(\kappa)}$, the iteration formula for $[\lambda_i]_{(\kappa+1)}$ can be expressed as

$$[\lambda_i]_{(\kappa+1)} = \frac{f_i\Big(\exp\Big([\mathbf{\Lambda}]_{(\kappa)}[t]\Big)[\mathbf{x}_{e,i}](0)\Big)}{\exp\Big([\mathbf{\Lambda}]_{(\kappa)}[t]\Big)[\mathbf{x}_{e,i}](0)}, \quad i = 1, \ldots, n. \tag{9}$$

The guaranteed state enclosure at the time instant $T = \sup([t])$ (the chosen end of the prediction window) is given by

$$\mathbf{x}_t^\star \in [\mathbf{x}_e](t) = \exp\Big([\mathbf{\Lambda}]T\Big)[\mathbf{x}_e](0), \tag{10}$$

where $[\mathbf{\Lambda}]$ is the final result of the iteration (9). For a suitable step size control strategy, allowing for a reduction of overestimation in the computed solutions for systems with non-negligible nonlinearities, the reader is referred to [11, Sec. III.C].

2.3 Design of the Subsidiary Robustly Stabilizing Feedback Controller

To design a linear, robustly stabilizing subsidiary feedback controller

$$\mathbf{u}_{\mathrm{fb}}(\mathbf{x}_t) = -\mathbf{K}\mathbf{x}_t, \tag{11}$$

we assume that the state equations

$$\dot{\mathbf{x}}_t = \mathbf{f}(t, \mathbf{x}_t, \mathbf{u}, \mathbf{p}) \tag{12}$$

can be reformulated into a quasi-linear form

$$\dot{\mathbf{x}}_t = \mathbf{A}(\mathbf{x}_t, \mathbf{u}, \mathbf{p})\mathbf{x}_t + \mathbf{B}(\mathbf{x}_t, \mathbf{p})\mathbf{u}. \tag{13}$$

As in the previous subsection, we assume for simplicity of the notation that the state space has been translated so that $\mathbf{x} = \mathbf{0}$ corresponds to the desired equilibrium.

Then, a robust linear state feedback controller (11) can be designed by a linear matrix inequality approach on the basis of the Lyapunov function candidate

$$V(\mathbf{x}_t) = \mathbf{x}_t^T \mathbf{P} \mathbf{x}_t \tag{14}$$

with the yet unknown symmetric, positive-definite matrix $\mathbf{P} = \mathbf{P}^T \succ 0$. For asymptotic stability, the property

$$\dot{V}(\mathbf{x}_t) < 0 \tag{15}$$

needs to hold for $\mathbf{x}_t \neq \mathbf{0}$. To ensure a minimum decay rate γ, this inequality can be replaced by

$$\dot{V}(\mathbf{x}) \leq -\gamma V(\mathbf{x}) \quad \text{with} \quad \gamma > 0. \tag{16}$$

Assuming further that the quasi-linear system model can be embedded into a convex polytopic uncertainty representation

$$\mathcal{D} = \left\{ [\mathbf{A}(\xi), \mathbf{B}(\xi)] \mid [\mathbf{A}(\xi), \mathbf{B}(\xi)] = \sum_{v=1}^{n_v} \xi_v \, [\mathbf{A}_v, \mathbf{B}_v,] \, ; \sum_{v=1}^{n_v} \xi_v = 1; \xi_v \geq 0 \right\}, \tag{17}$$

the bilinear matrix inequalities ($v = 1, \ldots, n_v$)

$$(\mathbf{A}_v - \mathbf{B}_v \mathbf{K})^T \, \mathbf{P} + \mathbf{P} \, (\mathbf{A}_v - \mathbf{B}_v \mathbf{K}) \prec 0 \; , \quad \mathbf{P} \succ 0 \tag{18}$$

need to be solved for the state-independent gain $\mathbf{K}$ to ensure asymptotic stability according to (15). This is typically done by means of a linearizing change of variables such as described in [21].

The more strict condition (16) is satisfied if

$$(\mathbf{A}_v - \mathbf{B}_v \mathbf{K})^T \, \mathbf{P} + \mathbf{P} \, (\mathbf{A}_v - \mathbf{B}_v \mathbf{K}) \prec 2\gamma \mathbf{P} \; , \quad \mathbf{P} \succ 0 \tag{19}$$

holds.

A drawback of this polytopic model approach is a certain degree of conservativeness introduced by treating all matrix entries as independent. This can be reduced by a norm-bounded uncertainty representation similarly used in [17].

In this case, robust asymptotic stability is achieved by satisfying the matrix inequality

$$\begin{aligned} &\begin{bmatrix} \mathbf{A}_{\text{nom}} \mathbf{P} - \mathbf{B}_{\text{nom}} \mathbf{Z} + \mathbf{P} \mathbf{A}_{\text{nom}}^T - \mathbf{Z}^T \mathbf{B}_{\text{nom}}^T & \mathbf{P} \mathbf{N}^T + \mathbf{Z}^T \mathbf{D}_{12}^T \\ \mathbf{N} \mathbf{P} + \mathbf{D}_{12} \mathbf{Z} & -\mu \mathbf{I} \end{bmatrix} \\ &+ \mu \begin{bmatrix} \mathbf{M} \mathbf{M}^T & \mathbf{M} \mathbf{Q}^T \\ \mathbf{Q} \mathbf{M}^T & \mathbf{Q} \mathbf{Q}^T \end{bmatrix} \prec 0 \end{aligned} \tag{20}$$

with $\mathbf{A}_{\text{nom}} = \text{mid}([\mathbf{A}]), \mathbf{B}_{\text{nom}} = \text{mid}([\mathbf{b}]), \mathbf{N} = \text{rad}([\mathbf{A}]), \mathbf{M} = \mathbf{I}, \mathbf{Q} = \mathbf{0}$, $\mathbf{D}_{12} = \text{rad}([\mathbf{B}]), \mathbf{P} \succ 0, \mathbf{K} = \mathbf{Z} \mathbf{P}^{-1}$, where $[\mathbf{A}]$ and $[\mathbf{B}]$ represent interval enclosures of the respective matrices in the polytopic model (17).

Remark. A means for further reduction of conservativeness, to be investigated in future work in combination with the validated NMPC, is the use of parameter-dependent Lyapunov function candidates, leading typically to larger regions of attraction for the equilibrium to be stabilized. In addition, it can be expected that parameter-dependent Lyapunov functions will allow for a more efficient use of the control effort [21]. Moreover, approaches for introducing hard saturations of the control signal and its variations rates as described in [13] can be investigated in future work.

Using the linear matrix inequality approach above, the following conclusions can be drawn:

- The feedforward term $\mathbf{u}_{\text{ff}}$ is mandatory for states outside the polytopic domain (17), where the stability of the feedback controller is not proven and this control part is, therefore, deactivated;
- The feedback controller can be activated as soon as states corresponding to the interior of the polytope (17) are attained;
- The exponential enclosure approach can be expected to find contracting solutions in the interior of this polytope, especially in combination with the comparison lemma [12] detailed subsequently.

The comparison lemma can be exploited to compute bounds for the Lyapunov function $V(\mathbf{x}_t)$ according to

$$\lambda_{\min}(\mathbf{P})\|\mathbf{x}_t\|_2^2 \leq \mathbf{x}_t^T\mathbf{P}\mathbf{x}_t \leq \lambda_{\max}(\mathbf{P})\|\mathbf{x}_t\|_2^2, \tag{21}$$

$$0 \leq \mathbf{x}_t^T\mathbf{P}\mathbf{x}_t \leq \mathbf{x}^T(0)\mathbf{P}\mathbf{x}(0), \tag{22}$$

where $\lambda_{\min}(\mathbf{P})$ and $\lambda_{\max}(\mathbf{P})$ are the smallest and largest eigenvalues of the matrix $\mathbf{P} = \mathbf{P}^T \succ 0$.

The enclosure (21) can be refined to

$$\lambda_{\min}(\mathbf{P})\|\mathbf{x}_t\|_2^2 \leq \mathbf{x}_t^T\mathbf{P}\mathbf{x}_t \leq e^{-\gamma t}\lambda_{\max}(\mathbf{P})\|\mathbf{x}(0)\|_2^2 \tag{23}$$

by exploiting the decay rate defined in (16). It immediately leads to the a-priori state enclosures

$$\|\mathbf{x}\|_2 \leq \sqrt{\frac{\lambda_{\max}(\mathbf{P})}{\lambda_{\min}(\mathbf{P})}}e^{-\frac{\gamma}{2}t}\|\mathbf{x}(0)\|_2 \tag{24}$$

that can always be intersected with the exponential enclosures (6) during the iterative computation of the parameters $[\lambda_i]_{(\kappa+1)}$.

Remark. Pessimism in this a-priori enclosure can be reduced by a computation of $\mathbf{P}$ after an (approximate) decoupling of the quasi-linear state equations by means of a suitable change of coordinates.

Remark. Due to the fact that the validated NMPC approach described in further detail in the following section performs a bisection of the control intervals, it is always possible to initialize the exponential enclosures' iteration formula (9) with the result obtained for the non-bisected interval. This is an obvious result of the enclosure property of interval analysis and helps to speed up the iteration procedure.

3 Validated Nonlinear Model Predictive Control

The purpose of this section is to review the work conducted in [4] where a new validated NMPC was developed on the basis of a Runge–Kutta method for validated integration. The approach uses interval analysis tools to compute a guaranteed control sequence over a receding horizon, taking into account the bounded uncertainties in the parameters of the dynamic system model and the measured data. Control intervals are computed in such a way that convergence to the set-point interval is ensured (i.e., $\mathbf{x}_j \rightarrow [\mathbf{x}_\mathrm{r}], \ \ \forall j$, which must be included in the interior of the state box from which the polytopic uncertainty model has been constructed in the previous section), and all the state and input constraints are satisfied (i.e., $\mathbf{x}_i \in [\mathbf{x}_i]$ and $\mathbf{u}_j \in [\mathbf{u}_j], \ \ \forall i, j$). In summary, the proposed guaranteed NMPC encompasses two stages [4],

- **Filtering and branching:** This first step provides a sequence of guaranteed input interval boxes at each time-step k over the prediction horizon N_p, denoted as $[\mathbf{U}_k] = [\mathbf{u}_k] \times [\mathbf{u}_{k+1}] \times \ldots \times [\mathbf{u}_{k+N_\mathrm{p}-1}]$. Branching and filtering procedures allow the computation of safe input intervals along the receding time horizon that satisfy the state constraints (i.e., $\forall j, [\mathbf{x}_j] \subseteq [\mathbf{x}_{\min,j}, \mathbf{x}_{\max,j}]$, where $\mathbf{x}_{\min,j}$ and $\mathbf{x}_{\max,j}$ are the bounds for the admissible domain for each state variable) and ensure convergence to the reference interval[2] (i.e., $[\mathbf{x}_k] \rightarrow [\mathbf{x}_\mathrm{r}]$).

  From the methodological point of view, the state limits should be verified at each validated simulation of the dynamic model using the exponential enclosures technique. If these limits are not satisfied, the initial input interval is further bisected and the validated simulations are relaunched. Subintervals after the bisection are kept according to the following criteria for selection:

  1. A branch leading to unsafe states is eliminated, i.e., if

  $$[\mathbf{x}_{t+T_\mathrm{c}}] \cap [\mathbf{x}_\mathrm{min} \ ; \ \mathbf{x}_\mathrm{max}] = \emptyset;$$

  2. A branch leading to a state far from the reference interval $[\mathbf{x}_\mathrm{r}]$ is also eliminated. The same holds for candidates partially having a cost greater than the other branch(es).

[2] Although only temporally constant reference values are discussed subsequently, time-varying reference trajectories $[\mathbf{x}_{\mathrm{r},k}]$ can be handled by the same algorithm.

- **Interval optimization:** The optimization algorithm computes safe inputs over a finite time horizon by minimizing a newly formulated interval objective function. This function aims to reduce the norm of the input intervals and the error between the predicted and reference outputs as much as possible, resulting in the computation of a sub-optimal input box $[\mathbf{U}]_k^\star$.

4 Application: Control of an Inverted Pendulum

4.1 Dynamic Modeling of the Inverted Pendulum

The control framework based on validated simulations presented in this paper is applied to the stabilization of the nonlinear inverted pendulum shown in Fig. 3. The pendulum is actuated by a DC motor whose angular speed is the input variable.

Following an Euler–Lagrange equation-based modeling procedure as described, for example, in [7], the dynamics of the rotary nonlinear inverted pendulum can be described by the ODEs

$$\begin{cases} \dot{x}_1 = x_2, \\ \dot{x}_2 = \dfrac{1}{\Delta}\Big\{ -\mu_3\cos(x_3)\left(\mu_1\sin(x_3)\cos(x_3)x_2^2 + \Gamma_2 - \mu_g\sin(x_3)\right) + \\ \qquad\qquad \mu_4\left(\mu_3\sin(x_3)x_4^2 - \mu_1\sin(2x_3)x_2x_4 + \Gamma_1\right)\Big\}, \\ \dot{x}_3 = x_4, \\ \dot{x}_4 = \dfrac{1}{\Delta}\Big\{ \left(\mu_1\sin(x_3)^2 + \mu_2\right)\left(\mu_1\cos(x_3)\sin(x_3)x_2^2 + \Gamma_2 - \mu_g\sin(x_3)\right) - \\ \qquad\qquad \mu_3\cos(x_3)\left(\mu_3\sin(x_3)x_4^2 - 2\mu_1\cos(x_3)\sin(x_3)x_2x_4 + \Gamma_1\right)\Big\}, \end{cases} \tag{25}$$

where x_1 and x_2 are, respectively, the angular position and velocity of the rotatory arm. Likewise, x_3 and x_4 are the angle and angular velocity of the pendulum arm. All of these variables are summarized in the state vector $\mathbf{x} = [x_1, x_2, x_3, x_4] \in \mathbb{R}^4$; $\Gamma_i = f_{vi}\dot{x}_i$ is the viscous friction torque at the joint i. Finally, the following state- and parameter-dependent terms are included in the system model (25)

$$\Delta = -\mu_3^2\cos(x_3)^2 + \mu_1\mu_4\sin(x_3)^2 + \mu_2\mu_4,$$

$$\mu_1 = l_{\mathrm{p}}^2\left(\frac{m_{\mathrm{p}}}{4} + M\right), \quad \mu_2 = l_{\mathrm{a}}^2(m_{\mathrm{p}} + M) + \frac{J_{\mathrm{m}}}{N_{\mathrm{g}}^2} + J_{\mathrm{a}},$$

$$\mu_3 = l_{\mathrm{p}}l_{\mathrm{a}}\left(\frac{m_{\mathrm{p}}}{2} + M\right), \quad \mu_4 = l_{\mathrm{p}}^2\left(\frac{m_{\mathrm{p}}}{4} + M\right) + J_{\mathrm{p}}, \quad \mu_{\mathrm{g}} = \left(\frac{m_{\mathrm{p}}}{2} + M\right)l_{\mathrm{p}}g,$$

where m_{a} and J_{a} denote the horizontal arm's mass and its inertia, respectively. Similarly, the mass and inertia of the pendulum arm are given by m_{p} and J_{p}; M is the mass of the load attached to the pendulum arm, J_{m} is the DC motor inertia, and N_{g} its gear ratio; l_{a}, l_{p}, and r_0 are the system's geometric parameters, and g

is the gravitational acceleration. A guaranteed identification of these parameters was performed in [5] with the help of interval methods. The corresponding results are summarized in Tab. 1.

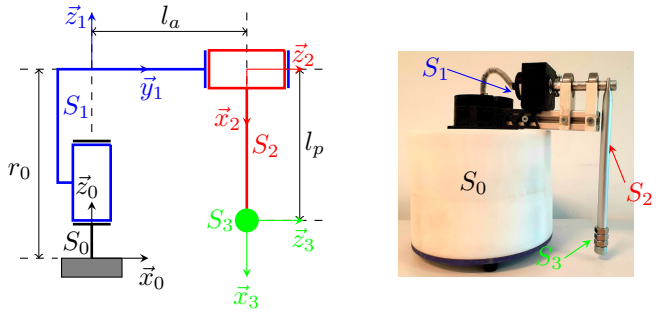

Figure 3: Left: Definition of links frame (configuration $x_1 = x_3 = 0°$); Right: representation of the nonlinear inverted pendulum.

Table 1: Interval bounds for the dynamic parameters of the inverted pendulum [5].

Symbol	**Interval Enclosure**	**Measurement Unit**
μ_1	$[9.63318 \cdot 10^{-4}\ ;\ 1.22604 \cdot 10^{-3}]$	$\mathrm{kg} \cdot \mathrm{m}^2$
μ_2	$[2.19585 \cdot 10^{-3}\ ;\ 2.79471 \cdot 10^{-3}]$	$\mathrm{kg} \cdot \mathrm{m}^2$
μ_3	$[7.227 \cdot 10^{-4}\ ;\ 8.833 \cdot 10^{-4}]$	$\mathrm{kg} \cdot \mathrm{m}^2$
μ_4	$[1.08271 \cdot 10^{-3}\ ;\ 1.37799 \cdot 10^{-3}]$	$\mathrm{kg} \cdot \mathrm{m}^2$
μ_g	$[6.24299 \cdot 10^{-2}\ ;\ 8.44641 \cdot 10^{-2}]$	$\mathrm{kg} \cdot \mathrm{m}^2 \cdot \mathrm{s}^{-2}$
f_{v_1}	$[0.043012\ ;\ 0.13002]$	$\mathrm{Nm} \cdot \mathrm{s} \cdot \mathrm{rad}^{-1}$
f_{v_2}	$[0.000454\ ;\ 0.001174]$	$\mathrm{Nm} \cdot \mathrm{s} \cdot \mathrm{rad}^{-1}$

4.2 Simulation Results

In [4], the NMPC was implemented for the following settings: prediction horizon $N_\mathrm{p} = 10$, control sampling time $T_\mathrm{c} = 16$ ms and the final time of the simulation $T_\mathrm{f} = 0.3$ s. The safety limits of all state variables are: $x_1 \in [-2\pi\ ;\ 2\pi]$, $x_2 \in [-52.4\ \mathrm{rad\ s^{-1}}\ ;\ 52.4\ \mathrm{rad\ s^{-1}}]$, $x_3 \in [-2\pi\ ;\ 2\pi]$, $x_4 \in [-100\ \mathrm{rad\ s^{-1}}\ ;\ 100\ \mathrm{rad\ s^{-1}}]$; the DC motor's torque is limited by the constraints $\tau \in [-8.05\ \mathrm{Nm}\ ;\ 8.05\ \mathrm{Nm}]$. The reference interval of the desired pendulum arm is $x_\mathrm{r} \in [\pi - 0.1\ ;\ \pi + 0.1]$. The tolerance parameter applied for the bisection procedure is adjusted as $tol = 0.25$. Since the filtering and branching algorithm begins from the admissible input domain

$[-8.05\ \text{Nm}\ ;\ 8.05\ \text{Nm}]$, it can lead to approximately 64^{10} branches with $N_\text{p} = 10$. The interval cost function is computed only in the optimization process using the weighting matrices $\mathbf{Q} = \text{diag}\,[1000, 1000, 1000, 1000]$ and $\mathbf{R} = 1$.

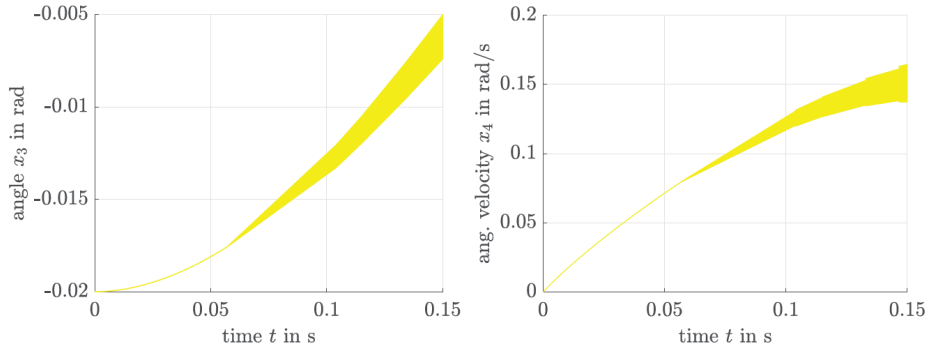

Figure 4: Simulation of the open-loop model using the exponential enclosure approach. Left: Pendulum angle $[\mathbf{x}_3]$; Right: Pendulum arm velocity $[\mathbf{x}_4]$.

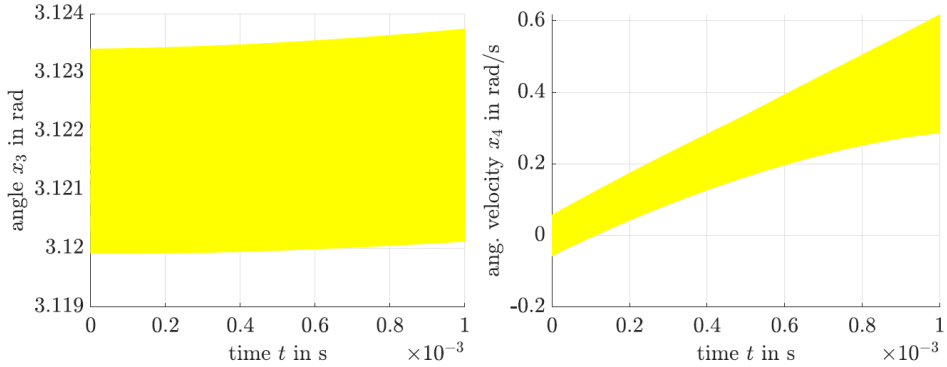

Figure 5: Simulation of the closed-loop model using the exponential enclosure approach. Left: Pendulum angle $[\mathbf{x}_3]$; Right: Pendulum arm velocity $[\mathbf{x}_4]$.

The exponential enclosure approach is now applied to the following two use cases:

1. Simulation of the open-loop dynamics (NMPC-based feedforward controller is switched off) and the pendulum's free motion shall be stabilized at the angle $x_3 = 0$;

2. Simulation of the influence of the subsidiary controller according to Sec. 2.3, after the NMPC has brought the pendulum arm close to its upright position.

For the simulation, the exponential enclosure technique has been implemented in the INTLAB library [20]. Figs. 4 and 5 display the open-loop and closed-loop simulation results of the combination of the exponential state enclosures approach with the control strategy. In Fig. 4, the length of the simulation time horizon is limited to half of the prediction window used for the NMPC.

As it can be seen in Fig. 4, the enclosures of the pendulum angle and its velocity, computed in the open-loop setting, converge to the open-loop stable equilibrium. Moreover, Fig. 5 shows the closed-loop system behavior, for which the computed enclosures of the pendulum angle and its velocity have a tolerable growth of pessimism over time. As already discussed in Sec. 2.3, future work will address the use of parameter-dependent Lyapunov functions for the subsidiary control design to enlarge the region of attraction of the desired equilibrium state and to limit the control effort by an explicit consideration of input and input rate constraints [13].

5 Conclusion and Future Works

This paper focuses on combining a reliable and validated nonlinear model predictive control (NMPC) with an exponential state enclosure technique which is advantageous for the simulation of uncertain dynamic systems with provably asymptotically stable dynamics. The efficiency and robustness of the proposed method were investigated through several numerical simulations using a nonlinear inverted pendulum.

In ongoing works, we focus on studying the following two issues: firstly, the extension of the exponential enclosure technique to ellipsoidal state domain representations, both for real- and complex-valued exponential enclosures, in combination with the extensions of the subsidiary control law discussed in this paper. Secondly, the application of the proposed approach on a real system. For the latter, it will also be required to estimate non-measured system states reliably by means of nonlinear robust observers which exploit interval methods not only to estimate bounds for the states at a specific point in time but also to reconstruct the influence of external disturbances.

References

[1] Alexandre dit Sandretto, J. and Chapoutot, A. DynIBEX: A differential constraint library for studying dynamical systems. In *Conference on Hybrid Systems: Computation and Control (HSCC 2016)*, 2016. https://hal.archives-ouvertes.fr/hal-01297273/file/dynibex-poster.pdf.

[2] Alexandre dit Sandretto, J. and Chapoutot, A. Validated explicit and implicit Runge–Kutta methods. *Reliable Computing electronic edition*, 22, 2016. https://www.cs.utep.edu/interval-comp/reliable-computing-22-pp-079-103.pdf.

[3] Allgöwer, F., Findeisen, R., and Nagy, Z. K. Nonlinear model predictive control: From theory to application. *Journal of the Chinese Institute of Chemical Engineers*, 35(3):299–316, 2004. DOI: 10.6967/JCICE.200405.0299.

[4] Fnadi, M. and Alexandre dit Sandretto, J. Experimental validation of a guaranteed nonlinear model predictive control. *Algorithms*, 14(8):248, 2021. DOI: 10.3390/a14080248.

[5] Fnadi, M., Alexandre dit Sandretto, J., Ballet, G., and Pribourg, L. Guaranteed identification of viscous friction for a nonlinear inverted pendulum through interval analysis and set inversion. In *2021 American Control Conference (ACC)*, pages 3920–3926, New Orleans, LA, USA, 2021. IEEE. DOI: 10.23919/ACC50511.2021.9483185.

[6] Fnadi, M., Du, W., Plumet, F., and Benamar, F. Constrained model predictive control for dynamic path tracking of a bi-steerable rover on slippery grounds. *Control Engineering Practice*, 107:104693, 2021. DOI: 10.1016/j.conengprac.2020.104693.

[7] Gäfvert, M. *Modelling the Furuta pendulum*. Department of Automatic Control, Lund Institute of Technology (LTH), 2016. https://lucris.lub.lu.se/ws/files/4453844/8727127.pdf (accessed: Feb. 12, 2023).

[8] Granvilliers, L. and Benhamou, F. Algorithm 852: Realpaver: An interval solver using constraint satisfaction techniques. *ACM Transactions on Mathematical Software (TOMS)*, 32(1):138–156, 2006. DOI: 10.1145/1132973.1132980.

[9] Henzinger, T. A., Horowitz, B., Majumdar, R., and Wong-Toi, H. Beyond HYTECH: Hybrid systems analysis using interval numerical methods. In *International Workshop on Hybrid Systems: Computation and Control*, pages 130–144. Springer, 2000. DOI: 10.1007/3-540-46430-1-14.

[10] Kapela, T., Mrozek, M., Wilczak, D., and Zgliczyński, P. CAPD:: DynSys: A flexible C++ toolbox for rigorous numerical analysis of dynamical systems. *Communications in nonlinear science and numerical simulation*, 101:105578, 2021. DOI: 10.1016/j.cnsns.2020.105578.

[11] Kersten, J., Rauh, A., and Aschemann, H. Application-based discussion of verified simulations of interval enclosure techniques. In *2019 24th International Conference on Methods and Models in Automation and Robotics (MMAR)*, pages 209–214, Międzyzdroje, Poland, 2019. DOI: 10.1109/MMAR.2019.8864673.

[12] Khalil, H. K. *Nonlinear systems*. Prentice-Hall, Upper Saddle River, NJ, 3rd edition, 2002. ISBN: 9780130673893.

[13] Lerch, S., Dehnert, R., Rosik, M., and Tibken, B. Minimizing oscillations for magnitude and rate-saturated discrete-time systems by a d_R region pole placement. In *Proceedings of the 10th International Conference on Systems and Control (ICSC)*, pages 244–249, Marseille, France, 2022. DOI: 10.1109/ICSC57768.2022.9993891.

[14] Lydoire, F. and Poignet, P. Nonlinear model predictive control via interval analysis. In *Proceedings of the 44th IEEE Conference on Decision and Control*, pages 3771–3776. IEEE, 2005. DOI: 10.1109/CDC.2005.1582749.

[15] Nedialkov, N. S., Jackson, K. R., and Corliss, G. F. Validated solutions of initial value problems for ordinary differential equations. *Applied Mathematics and Computation*, 105(1):21–68, 1999. DOI: 10.1016/S0096-3003(98)10083-8.

[16] Rauh, A. and Auer, E. Verified simulation of ODEs and DAEs in VALENCIA-IVP. *Reliable Computing*, 15(4):370–381, 2011. https://www.cs.utep.edu/interval-comp/reliable-computing-15-pp-370-381.pdf.

[17] Rauh, A., Bourgois, A., and Jaulin, L. Verifying provable stability domains for discrete-time systems using ellipsoidal state enclosures. *Acta Cybernetica*, 26(2):267–291, 2022. DOI: 10.14232/actacyb.293871.

[18] Rauh, A., Westphal, R., and Aschemann, H. Verified simulation of control systems with interval parameters using an exponential state enclosure technique. In *2013 18th International Conference on Methods & Models in Automation & Robotics (MMAR)*, pages 241–246, Międzyzdroje, Poland, 2013. IEEE. DOI: 10.1109/MMAR.2013.6669913.

[19] Rauh, A., Westphal, R., Aschemann, H., and Auer, E. Exponential enclosure techniques for initial value problems with multiple conjugate complex eigenvalues. In *International Symposium on Scientific Computing, Computer Arithmetic, and Validated Numerics*, pages 247–256. Springer, 2015. DOI: 10.1007/978-3-319-31769-4-20.

[20] Rump, S. INTLAB — INTerval LABoratory. In Csendes, T., editor, *Developments in Reliable Computing*, pages 77–104. Kluver Academic Publishers, 1999. DOI: 10.1007/978-94-017-1247-7_7.

[21] Scherer, C. and Weiland, S. Linear matrix inequalities in control. In Levine, W., editor, *Control System Advanced Methods*, The Electrical Engineering Handbook Series, pages 24–1—24–30. CRC Press, Boca Raton, 2nd edition, 2011. DOI: 10.1201/b10384.